

Detecting Initial System-Environment Correlations from a Single Observable

Ali Abu-Nada,¹ Russell Ceballos,^{2,3} and Lian-Ao Wu^{4,5}

¹*Sharjah Maritime Academy, United Arab Emirates*

²*Department of Physical Sciences, Olive-Harvey College,
City Colleges of Chicago, 10001 S Woodlawn Ave, Chicago, IL 60628, USA*

³*QuSTEAM Initiative, 510 Ronalds St., Iowa City, IA 52245, USA*

⁴*Department of Physics, University of the Basque Country UPV/EHU, 48080 Bilbao, Spain*

⁵*EHU Quantum Center, University of the Basque Country UPV/EHU, Leioa, Biscay 48940, Spain*

(Dated: February 24, 2026)

We address the problem of detecting initial system–environment correlations when the environment is not directly accessible. Most existing approaches rely on full state tomography or multiple system preparations, which can be experimentally demanding.

We show that, for a known interaction, it can be sufficient to monitor a single expectation value of the system. Focusing on a qubit interacting with an environment via isotropic Heisenberg exchange, we derive exact bounds on the signal $z(t) = \langle \sigma_z^S \rangle(t)$ that hold for all factorized initial states. These bounds define a *factorized envelope*: if an observed trajectory exits this envelope at any time, initial system–environment correlations are certified.

From a reduced-dynamics perspective, the envelope admits a clear operational interpretation as the admissible region generated by the standard product assignment (embedding) map, which serves as a null model for uncorrelated preparations. Envelope violations therefore rule out the entire product-assignment class using only a single calibrated observable.

We illustrate the method using three families of correlated initial states and observe clear envelope violations, including cases in which the reduced system state is maximally mixed. We further show that the same single-observable logic extends to an exactly solvable pure-dephasing spin–boson model with an infinite environment, where factorized initial states generate a simple coherence envelope whose violation certifies initial correlations. Overall, our results demonstrate that single-axis measurements, combined with a one-time calibration of $\rho_S(0)$, can certify initial system–environment correlations without tomography or environment access.

I. INTRODUCTION

Quantum technologies exploit intrinsically quantum resources, such as superposition and entanglement, to achieve tasks that are impossible classically [1, 2]. In realistic scenarios, however, a controllable system S is never perfectly isolated. Instead, it interacts with additional degrees of freedom E that we neither control nor directly monitor, and that we collectively refer to as the *environment*. The resulting open quantum dynamics may depend not only on noise generated during the evolution, but also on correlations that may already exist between S and E at the initial time [3–7]. Such initial correlations can invalidate the standard assumption that the reduced system dynamics form a completely positive (CP) dynamical map [3–5], and can obscure the identification of genuine memory effects, since increases in state distinguishability may originate from correlations at $t = 0$ rather than from information backflow [6, 7]. Importantly, whether initial system–environment correlations are detrimental or beneficial depends on the physical context and, in particular, on whether such correlations are uncontrolled or deliberately engineered. In this latter case, initial system–environment entanglement can in some settings be leveraged as a *resource* to mitigate effective decoherence during the evolution, allowing quantum computation to proceed approximately as if the system were effectively decoupled from its environment (see, e.g., Ref. [8]).

If both S and E are experimentally accessible, one could in principle detect and quantify correlations through joint measurements or full state tomography of SE [7, 9]. However, in many platforms the environment cannot be measured directly, which raises the central question:

To what extent can we detect initial system–environment correlations using only measurements on the system?

Several system-only strategies exist. One approach prepares multiple distinct initial system states and checks whether the effective environment state depends on the preparation, using process tomography or related reconstructions [7, 10]. Another widely used approach compares the reduced dynamics of two system states via trace distance or related distinguishability measures; increases in distinguishability can witness initial correlations or non-Markovian behavior [6, 11–16]. These methods are powerful but experimentally demanding, as they typically require (i) many different initial preparations or (ii) effective tomography of the reduced system. A complementary perspective assumes partial knowledge of the joint dynamics. If the interaction is known and the reduced state $\rho_S(t)$ can be reconstructed, one can test whether the observed evolution $\rho_S(0) \mapsto \rho_S(t)$ is compatible with any factorized initial state $\rho_S(0) \otimes \rho_E(0)$ [17, 18]. Recent theoretical results have strengthened this viewpoint by proving that, under broad conditions, initial correlations are always detectable from system-only data

if the joint dynamics is known and measurements are made at suitable times [19]. On the experimental side, system-only detection of initial entanglement with an inaccessible environment has been demonstrated using prior knowledge of the interaction, without performing full two-qubit tomography [20]. These advances underline both the conceptual relevance and the experimental feasibility of system-only detection of initial correlations.

Despite this progress, a common feature of most system-only protocols is their reliance on some form of reduced-state tomography. Even if the environment is never measured, the experimentalist typically needs to reconstruct the full Bloch vector of S by repeatedly measuring σ_x^S , σ_y^S , and σ_z^S . In many platforms, such as NMR ensembles, trapped ions, superconducting qubits, and NV centers—this tomographic overhead is nontrivial, and reducing the number of required measurement axes provides a practical advantage [6, 7, 9, 11, 15, 21, 22].

Foundational framing. When initial correlations may be present, a reduced evolution cannot, in general, be represented by a single completely positive (CP) map acting on the entire system state space without specifying how reduced states are embedded into the joint system-environment space [3–5]. This is naturally captured by an *assignment (embedding) map* \mathcal{A} , which assigns to each reduced input state a compatible joint state $\rho_{SE}(0) = \mathcal{A}(\rho_S(0))$. Different choices of \mathcal{A} generally lead to different reduced dynamics, and for correlated initial states a linear CP assignment typically exists only on a restricted subset of system states.

In this work, we do not attempt to reconstruct the assignment map from data. Instead, we adopt the standard *product assignment*, $\mathcal{A}_{\text{prod}}(\rho_S) = \rho_S \otimes \rho_E$, as a null hypothesis corresponding to uncorrelated preparations. We then ask which single-axis trajectories are compatible with this product embedding. This clarifies that our “factorized envelope” is precisely the admissible region associated with the product assignment, and that envelope violations certify that no uncorrelated (product) preparation can explain the observations.

In this work, we explore the extreme limit of this reduction and ask:

Can we certify initial system-environment correlations using only a single expectation value of a single system observable, measured along one fixed axis?

To address this question, we focus on the physical setting studied in Ref. [23], where a two-level system S interacts with a two-level environment E through the isotropic Heisenberg exchange Hamiltonian. We assume that the initial reduced state of the system, $\rho_S(0)$, is determined once through a calibration step (e.g., a single tomographic reconstruction at $t = 0$). After this calibration, we do not reconstruct $\rho_S(t)$ at later times; instead, we perform only one type of system measurement: the expectation value $z(t) = \langle \sigma_z^S \rangle(t)$, estimated experimentally by repeated projective measurements of σ_z^S . In other

words, after the initial calibration, we restrict ourselves to a *single observable along a single axis*.

A key objective of this work is to construct both a *mathematical* and a *geometrical* theory for the quantity $z(t)$ under this minimal measurement setting. The mathematical formulation expresses $z(t)$ in closed form, as an explicit function of the Heisenberg exchange parameters, the initial Bloch vector of the system, and the (unknown) Bloch vector of the environment. This formulation allows us to determine, for each time t , the exact range of possible values that $z(t)$ can take when the global initial state is factorized. At the same time, the geometrical formulation reveals that the Heisenberg exchange interaction generates a highly structured motion of the system Bloch vector: starting from $\rho_S(0)$, the reduced Bloch vector traces a partial-swap trajectory between the Bloch vectors of S and E . From this perspective, $z(t)$ is simply the time-dependent z -component of a rotating and contracting Bloch vector moving on the sphere along a well-defined curve. These two viewpoints—analytic and geometric—complement each other, and together they provide a transparent and intuitive understanding of the problem.

The central result emerging from this analysis is the following. If the initial joint state is factorized, $\rho_{SE}(0) = \rho_S(0) \otimes \rho_E(0)$, then for every time t the quantity $z(t)$ must lie inside a closed and analytically computable interval $\mathcal{R}(t) = [z_{\min}(t), z_{\max}(t)]$, which we call the *factorized envelope*. This envelope arises because, under the exchange interaction, every possible environment Bloch vector produces a distinct partial-swap curve, and the extremal values of $z(t)$ over all such curves define the upper and lower boundaries of $\mathcal{R}(t)$. If an experimentally observed trajectory $\tilde{z}(t)$ ever exits this envelope at any time, then no product initial state of the form $\rho_S(0) \otimes \rho_E(0)$ can explain the data, and initial system-environment correlations are therefore certified in a one-sided and device-friendly manner.

This approach combines several attractive features. First, it is mathematically exact: the envelope $\mathcal{R}(t)$ admits a closed-form expression and does not rely on numerical optimization or reconstruction procedures. Second, it has a clear geometrical meaning, which makes the witness both intuitive to interpret and visually compelling. Third, it uses only a single observable, σ_z^S , measured along a single axis, after a one-time calibration of $\rho_S(0)$. To our knowledge, this represents one of the most measurement-efficient system-only methods for certifying initial correlations under a known interaction model.

We do not claim that a single observable will suffice for arbitrary system-environment interactions; rather, we show that in the isotropic Heisenberg exchange model, a single calibrated observable already carries enough information to certify initial correlations.

Our main contributions are: (i) an analytically tractable and experimentally friendly construction of the factorized envelope $\mathcal{R}(t)$ for the isotropic Heisenberg exchange model; (ii) a minimal-observable, one-sided witness for

initial system-environment correlations based solely on measurements of σ_z^S ; and (iii) demonstrations of this witness on representative families of initial states originally examined in Ref. [23].

While much of our analysis focuses on a minimal two-qubit exchange model, we also demonstrate that the proposed witness is not an artifact of a finite environment by applying it to an exactly solvable infinite-bath dephasing model.

The rest of the paper is organized as follows. In Sec. II, we describe the protocol from an operational experimental perspective. In Sec. III, we introduce the model and develop both the mathematical and geometrical formulations of $z(t)$, including the reduced-dynamics assignment-map viewpoint. In Sec. IV, we derive the closed-form extremal values that define the factorized envelope for the isotropic Heisenberg exchange. In Sec. VI, we apply the witness to several families of correlated and uncorrelated initial states and illustrate its performance. In Sec. VII, we extend the single-observable witness to an exactly solvable pure-dephasing spin-boson model with an infinite environment, thereby demonstrating that the approach is not restricted to finite-dimensional environments. We conclude with a brief discussion.

II. PROCEDURE

In this section we describe the protocol in an operational manner, emphasizing how it is implemented in practice and how the resulting data are interpreted. We clearly separate what is done *in the laboratory* from what is done *in theory* to interpret the experimental data.

What is the basic idea?

When a quantum system interacts with an environment, correlations can appear in two different ways:

- correlations can be *created during the evolution*, even if the system and environment were initially uncorrelated;
- correlations can already *exist at the initial time*, before the evolution begins.

In this work we focus on the second case: *how can we tell whether correlations were already present at the initial time, using measurements on the system only?*

We assume that the interaction Hamiltonian H is known, and that the initial state of the system $\rho_S(0)$ can be calibrated once. After that, we only measure a single observable of the system, $z(t) = \langle \sigma_z^S \rangle(t)$.

The key question is therefore:

Given the calibrated system state $\rho_S(0)$ and a known interaction H , which values of $z(t)$ are possible if the initial state was uncorrelated?

If we can determine this range, then any experimentally observed value outside it proves that the initial state must have been correlated.

For the isotropic Heisenberg exchange, we show that all uncorrelated (product) initial states lead to values of $z(t)$ inside a time-dependent interval,

$$\mathcal{R}(t) = [z_{\min}(t), z_{\max}(t)], \quad (1)$$

which we call the *factorized envelope*.

Experimental protocol (Steps 1-3)

The first three steps describe only what the experimentalist does in the laboratory. At this stage, no assumption is made about whether the system and environment are correlated.

Step 1: Calibrate the system state.

Prepare the system qubit S in a known reduced state,

$$\rho_S(0) = \frac{1}{2}(\mathbb{I} + \vec{s} \cdot \vec{\sigma}), \quad (2)$$

where $\vec{s} = (s_x, s_y, s_z)$ is the Bloch vector. The vector \vec{s} is determined in a separate calibration run, for example by performing tomography at time $t = 0$.

This calibration is done only once. Afterward, no further tomography is required. The environment E starts in some unknown state $\rho_E(0)$, which may or may not be correlated with the system.

Step 2: Let the system and environment interact.

In each run of the experiment, the joint system starts in some physical state $\rho_{SE}(0)$ whose system marginal is the calibrated $\rho_S(0)$. The joint evolution is governed by the known Hamiltonian H ,

$$\rho_{SE}(t) = U(t) \rho_{SE}(0) U^\dagger(t), \quad U(t) = e^{-iHt}. \quad (3)$$

Operationally, the experimentalist simply prepares the same initial state as reproducibly as possible and allows the system and environment to interact for a time t .

Step 3: Measure a single observable.

For a chosen evolution time t , the experiment is repeated many times:

1. prepare the same initial joint state;
2. let it evolve for time t ;
3. measure σ_z^S on the system.

Averaging the measurement outcomes gives

$$z(t) = \langle \sigma_z^S \rangle(t) = \text{Tr}_S[\rho_S(t) \sigma_z^S], \quad (4)$$

where $\rho_S(t) = \text{Tr}_E[\rho_{SE}(t)]$. Only this single observable is measured, and the measurement axis is fixed throughout the experiment.

Theoretical analysis (Steps 4-5)

We now explain how the experimental data are interpreted.

Step 4: Define the uncorrelated reference model.

To test whether the data are compatible with an uncorrelated preparation, we introduce a *theoretical null hypothesis*. We assume that the initial joint state was uncorrelated and given by $\rho_{SE}(0) = \rho_S(0) \otimes \rho_E(0)$, where $\rho_E(0)$ is arbitrary.

This assumption corresponds to the standard *product assignment map*, which embeds the calibrated system state into a joint state assuming no initial correlations.

Under this assumption, different environment states lead to different trajectories $z(t)$. The set of all values obtainable in this way defines the factorized envelope,

$$\mathcal{R}(t) = \left\{ z(t) \mid \rho_{SE}(0) = \rho_S(0) \otimes \rho_E(0) \right\} = [z_{\min}(t), z_{\max}(t)]. \quad (5)$$

For the isotropic Heisenberg exchange, the bounds $z_{\min}(t)$ and $z_{\max}(t)$ can be computed analytically, as shown in Sec. IV.

Step 5: Compare theory and experiment.

Finally, the experimentally measured value $\tilde{z}(t)$ is compared with the theoretical interval $\mathcal{R}(t)$. If for some time t^* one finds

$$\tilde{z}(t^*) \notin \mathcal{R}(t^*),$$

then no uncorrelated (product) initial state can explain the observation. This certifies the presence of initial system-environment correlations.

Figure 1 provides a schematic illustration of the factorized envelope and how an experimentally observed trajectory can certify initial correlations by exiting this admissible region.

III. MODEL AND DEFINITIONS

We now formalize the setting and notation.

We consider a system qubit S and an environment qubit E with joint Hilbert space

$$\mathcal{H}_{SE} = \mathcal{H}_S \otimes \mathcal{H}_E, \quad \dim \mathcal{H}_S = \dim \mathcal{H}_E = 2. \quad (6)$$

The initial joint state $\rho_{SE}(0)$ may be either

$$\rho_{SE}(0) = \rho_S(0) \otimes \rho_E(0) \quad (\text{factorized}), \quad (7)$$

or

$$\rho_{SE}(0) \neq \rho_S(0) \otimes \rho_E(0) \quad (\text{correlated}), \quad (8)$$

where the latter may contain classical and/or quantum correlations, including entanglement.

The joint evolution is generated by a known Hamiltonian H on \mathcal{H}_{SE} , with unitary $U(t) = e^{-iHt}$ and

$$\rho_{SE}(t) = U(t)\rho_{SE}(0)U^\dagger(t). \quad (9)$$

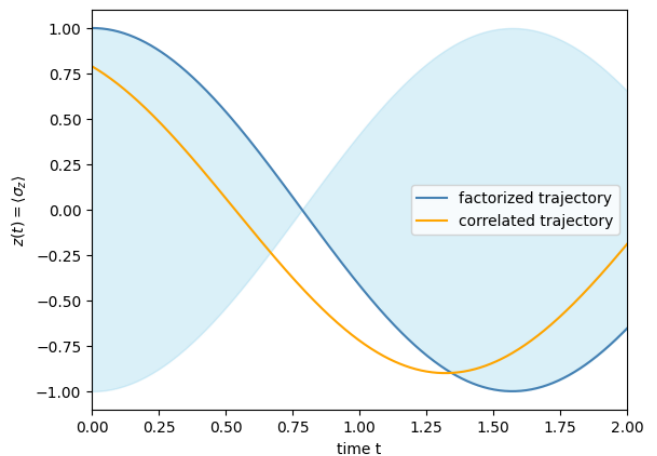


FIG. 1. Illustration of the factorized-envelope witness. The shaded region represents the factorized envelope $\mathcal{R}(t) = [z_{\min}(t), z_{\max}(t)]$, containing all trajectories $z(t) = \langle \sigma_z^S \rangle(t)$ obtainable from factorized initial states $\rho_{SE}(0) = \rho_S(0) \otimes \rho_E(0)$. The blue curve shows a representative factorized trajectory lying entirely inside the envelope, while the orange curve corresponds to a correlated initial state that exits the envelope, thereby certifying initial system-environment correlations.

The reduced state of the system is

$$\rho_S(t) = \text{Tr}_E[\rho_{SE}(t)]. \quad (10)$$

The calibrated initial state of S is written in Bloch form as

$$\rho_S(0) = \frac{1}{2}(\mathbb{I} + \vec{s} \cdot \vec{\sigma}), \quad |\vec{s}| \leq 1, \quad (11)$$

where $\vec{\sigma} = (\sigma_x, \sigma_y, \sigma_z)$ is the Pauli vector and $\vec{s} \in \mathbb{R}^3$ is the initial Bloch vector. At time t the reduced state is

$$\rho_S(t) = \frac{1}{2}(\mathbb{I} + \vec{s}(t) \cdot \vec{\sigma}), \quad |\vec{s}(t)| \leq 1, \quad (12)$$

with Bloch vector $\vec{s}(t) = (s_x(t), s_y(t), s_z(t))$.

The quantity accessible in our protocol is the single expectation value

$$z(t) = \langle \sigma_z^S \rangle(t) = \text{Tr}_S[\rho_S(t) \sigma_z^S] = \text{Tr}_S[\rho_S(0) \sigma_z^S(t)] = s_z(t), \quad (13)$$

the z -component of the system Bloch vector. In the second equality we use the Schrödinger picture, in which the state evolves and the observable is fixed; in the third equality we use the Heisenberg picture, in which the state is kept fixed and the observable evolves as $\sigma_z^S(t) = U^\dagger(t)\sigma_z^S U(t)$. Both descriptions are mathematically equivalent and refer to the same experimental procedure described in Sec. II: repeated preparation of $\rho_S(0)$, evolution under H , projective measurement of σ_z^S , and averaging of the outcomes. Our protocol never requires reconstructing $\rho_S(t)$ at intermediate times; after the one-time calibration of $\rho_S(0)$, all subsequent information enters through the single time-dependent observable $z(t)$.

When the initial state is factorized, we may write the environment as

$$\rho_E(0) = \frac{1}{2}(\mathbb{I} + \vec{e} \cdot \vec{\sigma}), \quad |\vec{e}| \leq 1, \quad (14)$$

but in the protocol we never need to know \vec{e} explicitly.

For each fixed t we define the set of all values of $z(t)$ obtainable from factorized initial states with the given calibration:

$$\mathcal{R}(t) = \{z(t) \mid \rho_{SE}(0) = \rho_S(0) \otimes \rho_E(0)\}. \quad (15)$$

Our main technical goal is to compute $\mathcal{R}(t)$ explicitly for the isotropic exchange Hamiltonian and to show that it is always an interval

$$\mathcal{R}(t) = [z_{\min}(t), z_{\max}(t)]. \quad (16)$$

Explicit formulas for $z_{\min}(t)$ and $z_{\max}(t)$ are obtained in Sec. IV.

A. Reduced-dynamics viewpoint: assignment maps and the product admissible set

A reduced system trajectory is ultimately generated by a joint unitary evolution on SE followed by a partial trace. When initial correlations may be present, a key foundational issue is that the reduced evolution cannot, in general, be represented by a single completely positive (CP) map on the full system state space without additional physical structure; instead, one must specify how a given reduced state $\rho_S(0)$ is embedded into the joint space. This is naturally captured by an *assignment map* (or embedding) \mathcal{A} , which assigns to each reduced input state a compatible joint state,

$$\rho_{SE}(0) = \mathcal{A}(\rho_S(0)), \quad (17)$$

and generates the reduced dynamics

$$\rho_S(t) = \text{Tr}_E[U(t)\mathcal{A}(\rho_S(0))U^\dagger(t)]. \quad (18)$$

In general, \mathcal{A} need not be unique, and physical consistency requirements may restrict the *domain* on which a given reduced description is valid. A useful structural condition is *G-consistency*: for a specified set of allowed global unitaries G , different joint states that share the same reduced state must induce the same reduced evolution under all $U \in G$, ensuring that the reduced dynamics are well defined on the chosen domain (see, e.g., Ref. [24]).

In our protocol, we do *not* attempt to reconstruct $\rho_S(t)$ or infer \mathcal{A} in full generality. Instead, we fix the reduced input state $\rho_S(0)$ once by calibration and monitor only the single expectation value

$$z(t) = \text{Tr}_S[\rho_S(t)\sigma_z^S] = \text{Tr}_{SE}[\mathcal{A}(\rho_S(0))U^\dagger(t)(\sigma_z^S \otimes \mathbb{I})U(t)]. \quad (19)$$

This viewpoint makes clear that even without full tomography, one can define a sharp *compatibility set* for factorized preparations by restricting to the standard product assignment

$$\mathcal{A}_{\text{prod}}(\rho_S(0)) = \rho_S(0) \otimes \rho_E(0), \quad (20)$$

with arbitrary environment state $\rho_E(0)$. For fixed $\rho_S(0)$ and t , the set of all values of $z(t)$ obtainable from (20) is exactly the factorized admissible region,

$$\mathcal{R}(t) = \left\{z(t) \mid \rho_{SE}(0) = \rho_S(0) \otimes \rho_E(0)\right\}. \quad (21)$$

Because $z(t)$ is affine in the unknown environment parameters under the product assignment, $\mathcal{R}(t)$ is an interval $[z_{\min}(t), z_{\max}(t)]$ whose endpoints are achieved by pure environment states. If an observed trajectory leaves this interval at any time, then no product assignment (20) can explain the data, and the initial joint state must have contained correlations. In Sec. IV we compute $z_{\min/\max}(t)$ analytically for the isotropic Heisenberg exchange.

IV. HEISENBERG EXCHANGE DYNAMICS AND ENVELOPE

We now specialize to the isotropic Heisenberg exchange Hamiltonian

$$H_{\text{ex}} = J(\sigma_x^S \sigma_x^E + \sigma_y^S \sigma_y^E + \sigma_z^S \sigma_z^E) = J\vec{\sigma}_S \cdot \vec{\sigma}_E, \quad (22)$$

with factorized initial state

$$\rho_{SE}(0) = \rho_S \otimes \rho_E, \quad \rho_S = \frac{1}{2}(\mathbb{I} + \vec{s} \cdot \vec{\sigma}), \quad \rho_E = \frac{1}{2}(\mathbb{I} + \vec{e} \cdot \vec{\sigma}). \quad (23)$$

Proposition 1. *Under H_{ex} the reduced system Bloch vector at time t is*

$$\vec{s}(t) = c^2 \vec{s} + d^2 \vec{e} + 2cd(\vec{s} \times \vec{e}), \quad (24)$$

where $c = \cos(2Jt)$ and $d = \sin(2Jt)$.

Proof. Define the exchange operator

$$K = \vec{\sigma}_S \cdot \vec{\sigma}_E = \sigma_x^S \sigma_x^E + \sigma_y^S \sigma_y^E + \sigma_z^S \sigma_z^E. \quad (25)$$

Using

$$\sigma_j \sigma_k = \delta_{jk} \mathbb{I} + i \sum_{\ell} \varepsilon_{jk\ell} \sigma_\ell, \quad (26)$$

one finds

$$K^2 = 3\mathbb{I}_4 - 2K, \quad (27)$$

so K satisfies a quadratic polynomial and its exponential can be written (up to a global phase) as

$$U(t) = e^{-iH_{\text{ex}}t} = e^{-iJtK} = c\mathbb{I}_4 - idK, \quad (28)$$

with $c = \cos(2Jt)$ and $d = \sin(2Jt)$.

The evolved joint state is

$$\rho_{SE}(t) = U(t)(\rho_S \otimes \rho_E)U^\dagger(t). \quad (29)$$

Using the Bloch decomposition

$$\rho_S \otimes \rho_E = \frac{1}{4} \left(\mathbb{I} \otimes \mathbb{I} + \vec{s} \cdot \vec{\sigma} \otimes \mathbb{I} + \mathbb{I} \otimes \vec{e} \cdot \vec{\sigma} + \sum_{jk} s_j e_k \sigma_j \otimes \sigma_k \right) \quad (30)$$

and repeatedly applying (26) together with $\text{Tr}[\sigma_j] = 0$ and $\text{Tr}[\sigma_j \sigma_k] = 2\delta_{jk}$, one finds that the reduced state $\rho_S(t) = \text{Tr}_E[\rho_{SE}(t)] = \frac{1}{2}(\mathbb{I} + \vec{s}(t) \cdot \vec{\sigma})$ has Bloch vector

$$\vec{s}(t) = \alpha(t)\vec{s} + \beta(t)\vec{e} + \gamma(t)\vec{s} \times \vec{e} \quad (31)$$

for some scalar functions $\alpha(t), \beta(t), \gamma(t)$.

The coefficients are fixed by three special cases: (i) $\vec{e} = 0$ gives $\vec{s}(t) = c^2\vec{s}$, so $\alpha = c^2$, $\beta = 0$; (ii) $\vec{s} = 0$ gives $\vec{s}(t) = d^2\vec{e}$, so $\beta = d^2$; and (iii) choosing $\vec{s} = \hat{z}$, $\vec{e} = \hat{x}$ yields $\vec{s}(t) = (d^2, 2cd, c^2)$, which implies $\gamma = 2cd$. Substituting these into the general form completes the proof. \square

Taking the z -component of Eq. (24) gives

$$z(t) = c^2 s_z + d^2 e_z + 2cd(s_x e_y - s_y e_x), \quad (32)$$

where $\vec{s} = (s_x, s_y, s_z)$ and $\vec{e} = (e_x, e_y, e_z)$.

Lemma 2. Let $\vec{a} \in \mathbb{R}^3$ and $b \in \mathbb{R}$, and consider

$$f(\vec{e}) = \vec{a} \cdot \vec{e} + b, \quad |\vec{e}| \leq 1. \quad (33)$$

Then the extrema of f over the Bloch ball occur on $|\vec{e}| = 1$ and are

$$f_{\max/\min} = b \pm |\vec{a}|. \quad (34)$$

Proof. For any \vec{e} with $|\vec{e}| \leq 1$,

$$f(\vec{e}) - b = \vec{a} \cdot \vec{e} \leq |\vec{a}| |\vec{e}| \leq |\vec{a}|, \quad (35)$$

so $f(\vec{e}) \leq b + |\vec{a}|$. The upper bound is achieved for $\vec{e} = \vec{a}/|\vec{a}|$ when $\vec{a} \neq 0$. A symmetric argument with $\vec{e} = -\vec{a}/|\vec{a}|$ gives the lower bound $b - |\vec{a}|$. \square

Remark. Because $f(\vec{e})$ is affine in \vec{e} , its extrema over the Bloch ball occur on the boundary $|\vec{e}| = 1$. Thus pure environment states determine the extremal values, while mixed states yield intermediate values inside the interval.

Corollary 3. For fixed \vec{s} and t , all factorized initial states $\rho_{SE}(0) = \rho_S \otimes \rho_E$ evolving under H_{ex} satisfy

$$z_{\min}(t) \leq z(t) \leq z_{\max}(t), \quad (36)$$

where

$$z_{\max/\min}(t) = c^2 s_z \pm d \sqrt{d^2 + 4c^2(s_x^2 + s_y^2)}. \quad (37)$$

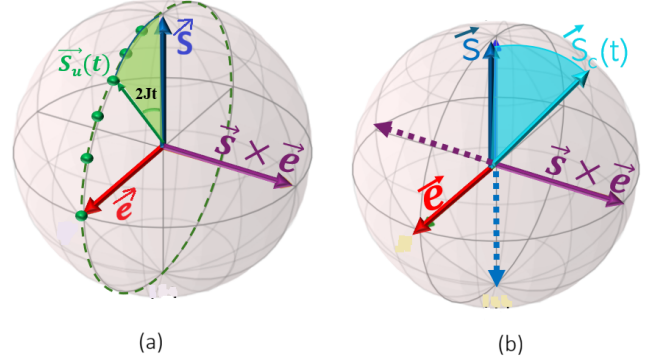


FIG. 2. (Color online) Geometric picture of exchange-driven Bloch-vector motion. (a) Factorized preparation: the system Bloch vector $\vec{s}_u(t)$ evolves in the plane spanned by the initial system vector \vec{s} and the environment vector \vec{e} , tracing a partial-swap arc with rotation axis $\vec{s} \times \vec{e}$. (b) Correlated preparation: initial correlations generate an additional component along $\vec{s} \times \vec{e}$, so the system trajectory $\vec{s}_c(t)$ leaves the \vec{s} - \vec{e} plane. This out-of-plane motion is incompatible with any factorized initial state with the same calibrated $\rho_S(0)$.

Proof. From Eq. (32) we write

$$z(t) = b(t) + \vec{a}(t) \cdot \vec{e}, \quad (38)$$

with

$$b(t) = c^2 s_z, \quad \vec{a}(t) = (-2cd s_y, 2cd s_x, d^2). \quad (39)$$

The norm is

$$\begin{aligned} |\vec{a}(t)|^2 &= 4c^2 d^2 (s_x^2 + s_y^2) + d^4 \\ &= d^2 \left[d^2 + 4c^2 (s_x^2 + s_y^2) \right]. \end{aligned} \quad (40)$$

Applying Lemma 2 with $b = b(t)$ and $\vec{a} = \vec{a}(t)$ gives

$$z_{\max/\min}(t) = b(t) \pm |\vec{a}(t)| = c^2 s_z \pm d \sqrt{d^2 + 4c^2 (s_x^2 + s_y^2)}. \quad (41)$$

\square

A. Geometric interpretation and partial swap

Figure 2 summarizes the key geometric difference between factorized and correlated initial preparations under exchange: factorized dynamics remain confined to the plane spanned by \vec{s} and \vec{e} , while correlations can produce an out-of-plane component along $\vec{s} \times \vec{e}$.

Equation (24) shows that, for factorized initial states, the system Bloch vector moves along a “partial-swap” trajectory connecting \vec{s} and \vec{e} :

- at $t = 0$ ($c = 1, d = 0$), $\vec{s}(t) = \vec{s}$;
- at $2Jt = \pi/2$ ($c = 0, d = 1$), $\vec{s}(t) = \vec{e}$;

- for $0 < t < \pi/2$, $\vec{s}(t)$ is a weighted combination of \vec{s} and \vec{e} plus a rotation generated by $\vec{s} \times \vec{e}$.

The cross-product term is orthogonal to the plane spanned by \vec{s} and \vec{e} and produces a rigid rotation around the axis $\vec{s} \times \vec{e}$. In other words, $\vec{s}(t)$ traces a circular arc in the \vec{s} - \vec{e} plane, centered on the axis $\vec{s} \times \vec{e}$, interpolating smoothly between the two Bloch vectors. This partial-swap motion is depicted in Fig. 2(a), where the uncorrelated trajectory $\vec{s}_u(t)$ lies entirely in the plane determined by \vec{s} and \vec{e} .

The same structure can also be expressed directly at the unitary level as

$$U(t) = \cos(2Jt) \mathbb{I} - i \sin(2Jt) \text{SWAP}, \quad (42)$$

up to an overall phase, where SWAP exchanges S and E . At $t = 0$ the evolution is the identity, at $2Jt = \pi/2$ it is (up to phase) a full SWAP, and for intermediate times it is a coherent superposition of identity and SWAP.

For factorized states, the reduced Bloch vector is confined to these partial-swap trajectories, and consequently $z(t) = s_z(t)$ is confined to the interval $[z_{\min}(t), z_{\max}(t)]$ derived in Corollary 3. When the initial state is correlated, additional contributions from the correlation tensor tilt the effective rotation axis and push $\vec{s}(t)$ out of the \vec{s} - \vec{e} plane, as illustrated by the correlated trajectory $\vec{s}_c(t)$ in Fig. 2(b). In this case, the resulting $z(t)$ can leave the factorized envelope, which is precisely the signature exploited by our single-observable witness.

V. WITNESS OF INITIAL CORRELATIONS

We can now state the witness formally.

Theorem 4 (Minimal-observable witness). *Let the system evolve under H_{ex} with known initial $\rho_S(0) = \frac{1}{2}(\mathbb{I} + \vec{s} \cdot \vec{\sigma})$. For each t , let $[z_{\min}(t), z_{\max}(t)]$ be the factorized envelope of Corollary 3. If for some t^* the experimentally observed value $\tilde{z}(t^*)$ satisfies*

$$\tilde{z}(t^*) \notin [z_{\min}(t^*), z_{\max}(t^*)], \quad (43)$$

then the initial joint state $\rho_{SE}(0)$ was not factorized. In particular, initial S - E correlations are certified.

Proof. Corollary 3 shows that every factorized state $\rho_{SE}(0) = \rho_S \otimes \rho_E$ with the given ρ_S produces $z(t)$ in the interval $[z_{\min}(t), z_{\max}(t)]$. Thus

$$\mathcal{R}(t) = \left\{ z(t) \mid \rho_{SE}(0) = \rho_S \otimes \rho_E \right\} = [z_{\min}(t), z_{\max}(t)]. \quad (44)$$

If $\tilde{z}(t^*)$ lies outside this interval, there is no product state consistent with the observation at t^* , so $\rho_{SE}(0)$ cannot be factorized. \square

VI. EXAMPLES: THREE CANONICAL INITIAL STATES

In the protocol as implemented in the laboratory, only the reduced system state $\rho_S(0)$ is calibrated experimentally; the joint state $\rho_{SE}(0)$ is unknown and may or may not be correlated. In the following examples, by contrast, we *theoretically specify* a particular joint initial state $\rho_{SE}(0)$ in order to analyze the performance of the witness. The corresponding calibrated system state is always obtained as $\rho_S(0) = \text{Tr}_E[\rho_{SE}(0)]$, matching what an experimentalist would have determined in the initial calibration step. The subsequent comparison between the correlated trajectory $z^{(\text{corr})}(t)$ and the factorized envelope $\mathcal{R}(t)$ is therefore carried out using only system data and the known Hamiltonian, exactly as in the operational protocol.

We now illustrate the witness using the three families of initial states analyzed in Ref. [23]. In each case we:

1. specify the (possibly correlated) initial state $\rho_{SE}(0)$;
2. determine the calibrated reduced state $\rho_S(0)$ and its Bloch vector $\vec{s}(0)$;
3. compute the correlated trajectory $z^{(\text{corr})}(t)$; and
4. compare $z^{(\text{corr})}(t)$ with the factorized envelope $[z_{\min}(t), z_{\max}(t)]$.

Whenever $z^{(\text{corr})}(t)$ leaves the envelope, the witness detects initial correlations using only the single observable $z(t)$.

For convenience we parameterize time by $\alpha = Jt$, so that

$$c = \cos(2Jt) = \cos(2\alpha), \quad d = \sin(2Jt) = \sin(2\alpha).$$

A. Example 1: Maximally entangled Bell-like state

We first consider a maximally entangled initial state of S and E ,

$$\rho_{SE}(0) = |\Psi\rangle\langle\Psi|, \quad |\Psi\rangle = \frac{1}{\sqrt{2}}(|01\rangle + i|10\rangle). \quad (45)$$

Tracing out the environment gives a maximally mixed reduced state

$$\rho_S(0) = \text{Tr}_E[\rho_{SE}(0)] = \frac{1}{2} \mathbb{I}, \quad \vec{s}(0) = \vec{0}, \quad z(0) = 0. \quad (46)$$

Thus, based solely on system information at $t = 0$, this preparation is indistinguishable from an uncorrelated product state with the same $\rho_S(0)$.

Reduced system trajectory. To determine $\rho_S(t)$ under the isotropic exchange Hamiltonian $H_{\text{ex}} = J \vec{\sigma}_S \cdot \vec{\sigma}_E$, it is convenient to use the singlet-triplet basis, in which H_{ex}

is diagonal. Decomposing $|\Psi\rangle$ in this basis, evolving each component, and tracing out E yields

$$\rho_S(t) = \begin{pmatrix} p_0(t) & 0 \\ 0 & 1 - p_0(t) \end{pmatrix}, \quad p_0(t) = \frac{1}{2}(1 - \sin 4Jt). \quad (47)$$

Hence the correlated single-axis observable is

$$z^{(\text{corr})}(t) = \langle \sigma_z^S \rangle(t) = p_0(t) - [1 - p_0(t)] = -\sin(4Jt). \quad (48)$$

Factorized comparison envelope. To apply the witness, we compare $z^{(\text{corr})}(t)$ with the set of all factorized preparations that are consistent with the same calibrated $\rho_S(0) = \mathbb{I}/2$. For any such state, the initial system Bloch vector satisfies $\vec{s}(0) = \vec{0}$, so Eq. (32) reduces to

$$z(t) = d^2 e_z, \quad d = \sin(2Jt), \quad e_z \in [-1, 1]. \quad (49)$$

Optimizing over e_z yields the factorized envelope

$$z_{\min/\max}(t) = \pm \sin^2(2Jt), \quad (50)$$

and therefore every product initial state must satisfy

$$-\sin^2(2Jt) \leq z(t) \leq \sin^2(2Jt).$$

Witness violation and figure interpretation. Figure 3 compares the correlated trajectory $z^{(\text{corr})}(t)$ (black curve) with the factorized envelope $[z_{\min}(t), z_{\max}(t)]$ (blue shaded region). At the witness time $t^* = 3\pi/(8J)$,

$$\sin(4Jt^*) = -1, \quad \sin^2(2Jt^*) = \frac{1}{2},$$

so $z^{(\text{corr})}(t^*) = 1$ while every factorized initial state allows only $z(t^*) \in [-\frac{1}{2}, \frac{1}{2}]$. The red marker in Fig. 3 highlights this violation. Since no product initial state with the same calibrated $\rho_S(0)$ can reproduce this value, initial system-environment correlations are certified using only the single observable $z(t)$.

Experimental note. In practice, $z(t) = \langle \sigma_z^S \rangle(t)$ is obtained by repeatedly preparing the system and performing a projective measurement of σ_z^S at time t , then averaging the binary outcomes. This procedure uses only a single measurement axis and is standard in NMR, trapped ions, superconducting qubits, and NV centers.

B. Example 2: Mixture of a product state and an entangled state

We next consider a family of mixed initial states interpolating between a product state and the maximally entangled state of Example 1:

$$\rho_{SE}(0) = p |01\rangle\langle 01| + (1-p) |\Psi\rangle\langle \Psi|, \quad 0 \leq p \leq 1, \quad (51)$$

with $|\Psi\rangle$ as defined above. Tracing out the environment gives

$$\rho_S(0) = \begin{pmatrix} \frac{1+p}{2} & 0 \\ 0 & \frac{1-p}{2} \end{pmatrix}, \quad \vec{s}(0) = (0, 0, p), \quad z(0) = p, \quad (52)$$

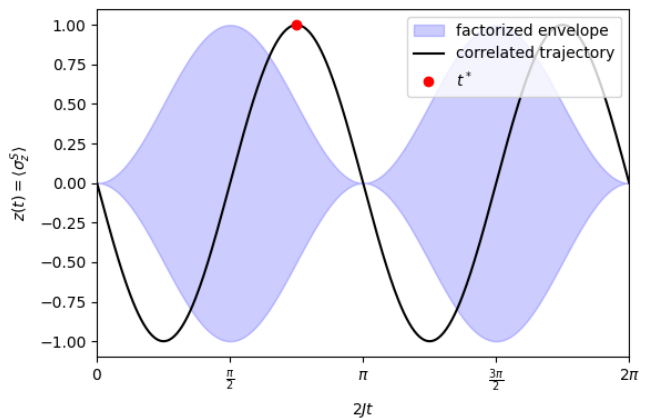


FIG. 3. (Color online) Example 1. The black curve shows the correlated trajectory $z^{(\text{corr})}(t) = -\sin(4Jt)$ for the maximally entangled initial state. The blue shaded region is the factorized envelope $z_{\min/\max}(t) = \pm \sin^2(2Jt)$ for all product states with $\rho_S(0) = \mathbb{I}/2$. At $t^* = 3\pi/(8J)$ (red marker), the correlated value lies outside the admissible region, certifying initial correlations using only $z(t)$.

so the calibrated system state contains a finite polarization p along z .

Correlated trajectory. Using the singlet-triplet decomposition as before, evolving under $H_{\text{ex}} = J \vec{\sigma}_S \cdot \vec{\sigma}_E$ and tracing out E yields the correlated single-axis observable

$$z^{(\text{corr})}(t) = p \cos(4Jt) + (p-1) \sin(4Jt), \quad (53)$$

which continuously connects to Example 1 when $p = 0$.

Factorized comparison envelope. To construct the witness, we compare $z^{(\text{corr})}(t)$ with all factorized initial states consistent with the same calibrated $\rho_S(0)$. For any such product state, $\vec{s}(0) = (0, 0, p)$, so Eq. (32) reduces to

$$z(t) = c^2 p + d^2 e_z, \quad e_z \in [-1, 1], \quad (54)$$

with $c = \cos(2Jt)$ and $d = \sin(2Jt)$. Optimizing over e_z yields the envelope

$$z_{\min/\max}(t) = \cos^2(2Jt)p \pm \sin^2(2Jt), \quad (55)$$

and therefore every factorized initial state with the same $\rho_S(0)$ must satisfy

$$\cos^2(2Jt)p - \sin^2(2Jt) \leq z(t) \leq \cos^2(2Jt)p + \sin^2(2Jt).$$

Witness violation. A convenient witness time is $t^* = 3\pi/(8J)$, for which

$$z^{(\text{corr})}(t^*) = 1 - p, \quad z_{\min/\max}(t^*) = \left[\frac{p-1}{2}, \frac{p+1}{2} \right].$$

Violation occurs when $1 - p > (p+1)/2$, i.e. for $p < 1/3$. Thus, for $0 \leq p < 1/3$, the correlated trajectory necessarily lies outside the factorized envelope at t^* , certifying initial S - E correlations. For larger p the mixture is dominated by the product component, and no violation occurs at this particular time (although it may occur at others).

Figure interpretation. Figure 4 shows the correlated trajectories $z^{(\text{corr})}(t)$ (black curves) together with the corresponding factorized envelopes (blue shaded regions) for three representative values of p . The panels illustrate how decreasing p increases the weight of the entangled component and eventually produces a clear envelope crossing. For $p = 0.6$ the correlated curve remains inside the envelope at t^* ; for $p = 0.2$ and $p = 0.1$ the correlated value at the red marker lies strictly outside the envelope, certifying initial correlations with a single observable.

C. Example 3: Mixture with the maximally mixed state

Finally, we consider a different type of mixture in which the entangled state of Example 1 is diluted by the maximally mixed two-qubit state:

$$\rho_{SE}(0) = p \frac{\mathbb{I}_4}{4} + (1-p) |\Psi\rangle\langle\Psi|, \quad 0 \leq p \leq 1, \quad (56)$$

where $|\Psi\rangle$ is the maximally entangled state used previously. Tracing out the environment yields

$$\rho_S(0) = p \frac{\mathbb{I}_2}{2} + (1-p) \frac{\mathbb{I}_2}{2} = \frac{\mathbb{I}_2}{2}, \quad (57)$$

so the calibrated system state is maximally mixed, with $\vec{s}(0) = \vec{0}$ and $z(0) = 0$, regardless of p .

Correlated trajectory. The maximally mixed part is invariant under all unitary dynamics and therefore does not contribute to $z(t)$. Only the entangled component evolves nontrivially, and using the result of Example 1 we obtain

$$z^{(\text{corr})}(t) = (p-1) \sin(4Jt), \quad (58)$$

which continuously interpolates between the fully entangled trajectory ($p = 0$) and a flat signal ($p = 1$).

Factorized comparison envelope. Since $\rho_S(0) = \mathbb{I}_2/2$ for all p , the factorized initial states have $\vec{s}(0) = \vec{0}$ and the envelope reduces to the same form as in Example 1:

$$z_{\text{min/max}}(t) = \pm \sin^2(2Jt). \quad (59)$$

Therefore, every factorized initial state compatible with the same calibration must satisfy

$$-\sin^2(2Jt) \leq z(t) \leq \sin^2(2Jt).$$

Witness violation and figure interpretation. A violation occurs whenever

$$|z^{(\text{corr})}(t)| = |1-p| |\sin(4Jt)| > \sin^2(2Jt). \quad (60)$$

Since $\sin^2(2Jt)$ can be made arbitrarily small while $|\sin(4Jt)|$ remains close to 1 (e.g., when $2Jt$ is close to but not exactly $\pi/2$), any $p < 1$ produces times at which the correlated trajectory exceeds the envelope. Thus, even though the reduced state is maximally mixed and

reveals no information at $t = 0$, suitably chosen single-axis measurements at later times can detect the hidden initial S - E correlations for all $p < 1$.

Figure 5 illustrates this behavior. The blue shaded regions indicate the factorized envelope, and the black curves show $z^{(\text{corr})}(t)$ for three representative values of p . For $p = 0.8$, the entangled component is weak and the correlated trajectory remains close to the envelope. For $p = 0.4$, clear excursions beyond the envelope appear, and for $p = 0.1$ the envelope violations are pronounced. As $p \rightarrow 1$, the state approaches the maximally mixed product state and the correlated signal becomes vanishingly small, consistent with the absence of detectable correlations.

VII. EXTENSION TO AN EXACTLY SOLVABLE INFINITE-BATH MODEL

While the isotropic Heisenberg exchange provides a minimal and fully controllable setting for developing the single-observable witness, it is natural to ask whether the same logic survives in more conventional open-system models with infinite environments. In this section, we demonstrate that the witness extends naturally to the exactly solvable pure-dephasing spin-boson model, which is a standard benchmark in the theory of open quantum systems.

A. Pure-dephasing spin-boson Hamiltonian

We consider the Hamiltonian [Eq. (4.28) of Ref. [1]]

$$H = \frac{\omega_0}{2} \sigma_z + \sum_k \omega_k b_k^\dagger b_k + \sigma_z \sum_k \left(g_k b_k^\dagger + g_k^* b_k \right), \quad (61)$$

where σ_z acts on the system qubit and $\{b_k, b_k^\dagger\}$ are bosonic operators describing an infinite environment. This model generates pure dephasing: the system populations remain constant, while the coherences decay in time. Importantly, the reduced dynamics admit a closed-form solution for factorized initial states, making this model analytically tractable.

B. Reduced dynamics for factorized initial states

Assuming an initially factorized state $\rho_{SE}(0) = \rho_S(0) \otimes \rho_E(0)$, the reduced system state at time t is given by

$$\rho_S(t) = \begin{pmatrix} \rho_{00}(0) & \rho_{01}(0) e^{-\Gamma(t)} \\ \rho_{10}(0) e^{-\Gamma(t)} & \rho_{11}(0) \end{pmatrix}, \quad (62)$$

where $\Gamma(t) \geq 0$ is the decoherence function determined by the bath spectral density and temperature. Its explicit form is not required for our purposes; the only properties we use are that $\Gamma(0) = 0$ and $e^{-\Gamma(t)} \in [0, 1]$ for all t .

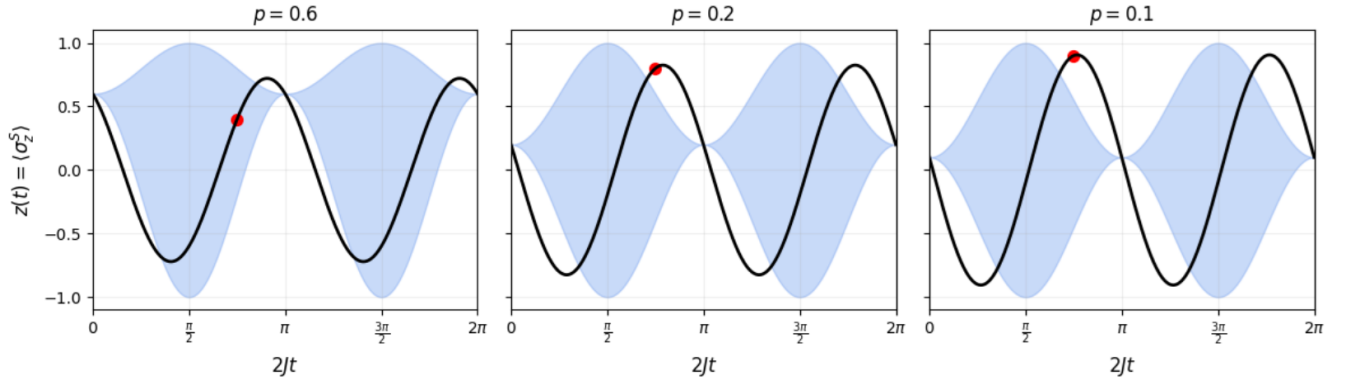


FIG. 4. (Color online) Example 2. The blue shaded region shows the factorized envelope $z_{\min/\max}(t) = \cos^2(2Jt)p \pm \sin^2(2Jt)$ for product initial states with the calibrated $\rho_S(0)$. The black curves show the correlated trajectories $z^{(\text{corr})}(t) = p \cos(4Jt) + (p-1)\sin(4Jt)$. Panels correspond to different values of p . For $p < 1/3$, the correlated trajectory leaves the envelope (red marker), certifying initial system–environment correlations using only $z(t)$.

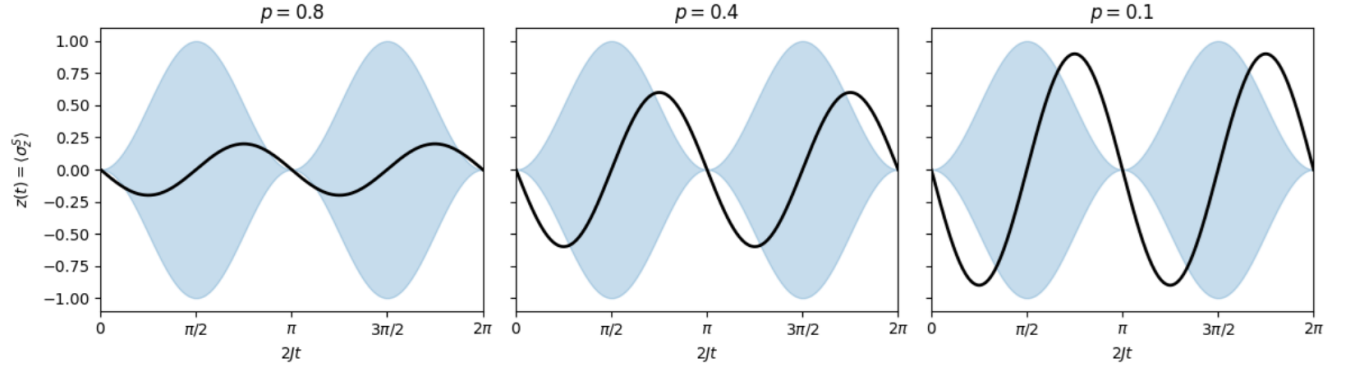


FIG. 5. (Color online) Example 3. The blue shaded region shows the factorized envelope $z_{\min/\max}(t) = \pm \sin^2(2Jt)$ for product initial states with the calibrated $\rho_S(0) = \mathbb{I}/2$. The black curves show the correlated trajectories $z^{(\text{corr})}(t) = (p-1)\sin(4Jt)$ for different values of p . For smaller p (stronger entangled component), the trajectories clearly leave the envelope, certifying initial S – E correlations even though the reduced state is maximally mixed at $t = 0$.

Since $\langle \sigma_z \rangle(t)$ is constant under pure dephasing, we focus on a single transverse observable,

$$x(t) = \langle \sigma_x \rangle(t) = \text{Tr}_S[\rho_S(t)\sigma_x]. \quad (63)$$

From Eq. (62), one obtains

$$x(t) = x(0)e^{-\Gamma(t)}, \quad (64)$$

where $x(0) = \langle \sigma_x \rangle(0)$ is fixed by the initial calibration of $\rho_S(0)$.

C. Factorized envelope and witness

For any factorized initial state consistent with the calibrated $\rho_S(0)$, the initial coherence satisfies $|x(0)| \leq 1$. Equation (64) therefore implies that all factorized preparations obey the bound

$$|x(t)| \leq e^{-\Gamma(t)}. \quad (65)$$

This inequality defines a time-dependent *factorized envelope* for the single observable $x(t)$ under the pure-dephasing dynamics. It represents the entire set of values compatible with the standard product assignment $\rho_{SE}(0) = \rho_S(0) \otimes \rho_E(0)$ for an infinite bosonic bath.

Unlike the exchange model, the pure-dephasing dynamics admit no further optimization over environmental degrees of freedom beyond the decoherence function $\Gamma(t)$. Consequently, the factorized envelope takes a particularly simple form, while any deviation from it directly reflects the presence of initial system–environment correlations.

If, for some time t^* , an experimentally observed value $\tilde{x}(t^*)$ violates Eq. (65), then no factorized initial state can account for the observation. Such a violation therefore certifies the presence of initial system–environment correlations using only a single system observable and without any access to the environment.

This example demonstrates that the single-observable witness is not restricted to finite environments or exchange-type interactions. Even in a paradigmatic

infinite-bath model with analytically solvable reduced dynamics, factorized initial states generate a sharply constrained admissible region for a single system observable. Initial correlations modify the coherence dynamics and can drive the signal outside this region, providing a clear and experimentally accessible signature of correlated preparations.

VIII. CONCLUSION

In this work we investigated how much information about initial system-environment correlations can be inferred from the dynamics of a single system observable, without access to the environment or full state tomography. Focusing on the isotropic Heisenberg exchange between two qubits, we showed that a one-time calibration of $\rho_S(0)$ followed by single-axis measurements of $z(t) = \langle \sigma_z^S \rangle(t)$ can already certify the presence of initial correlations.

The protocol rests on two structural ingredients of the Heisenberg model. First, for all factorized initial states, the reduced system Bloch vector follows an exactly solvable partial-swap trajectory whose projection onto the z -axis is highly constrained. Second, by optimizing over all product preparations consistent with the calibrated $\rho_S(0)$, we derived a closed-form envelope $[z_{\min}(t), z_{\max}(t)]$ that bounds every possible factorized trajectory. Any observed value $\tilde{z}(t)$ that escapes this envelope excludes all product initial states with the same $\rho_S(0)$ and therefore certifies initial S - E correlations.

Assignment-map interpretation. From a reduced-dynamics perspective, our witness tests compatibility with the standard product assignment map, which serves as a natural null model for uncorrelated preparations. The factorized envelope is precisely the admissible region generated by this product embedding, and envelope violations rule out the entire product-assignment hypothesis without reconstructing $\rho_S(t)$ or inferring an assignment map in general.

The geometric picture underlying the partial-swap constraint naturally explains why only certain single-axis trajectories are compatible with factorized states. In Appendix A we formalize this intuition by decomposing the correlation tensor and showing how correlated initial states produce an additional deviation term that moves the reduced Bloch vector off the partial-swap manifold.

We applied the witness to three representative families of correlated states—including mixtures with maximally mixed marginals—and found that suitable evolution times reveal clear envelope violations. These examples highlight the central message of this work: initial correlations can remain completely invisible at $t = 0$ yet become detectable through the time series of a single system observable under a known interaction.

The approach is relevant for experimental platforms in which only one measurement axis is naturally available or tomographic reconstruction is costly. More broadly,

it suggests a program of “single-observable witnesses” for other interactions and higher-dimensional environments, including anisotropic exchange, pure dephasing, Jaynes-Cummings models, and multi-qubit settings. Taken together, our results show that surprisingly minimal measurement resources can provide nontrivial insight into initial system-environment correlations, bringing theoretical detectability closer to experimental feasibility.

Finally, we emphasize that we do not claim that a single observable will suffice for arbitrary system-environment interactions. Our results demonstrate that, for the isotropic Heisenberg exchange between two qubits, a single calibrated observable already carries enough information to certify initial correlations.

Finally, we showed that the single-observable witness is not restricted to finite environments or exchange-type interactions. By applying the same logic to the exactly solvable pure-dephasing spin-boson model with an infinite bath, we found that factorized initial states give rise to a simple but sharp coherence envelope, whose violation unambiguously signals initial correlations. This demonstrates that the witness captures a structural feature of correlated preparations rather than an artifact of finite-dimensional environments.

ACKNOWLEDGEMENT

L.-A.W. is supported by the Basque Country Government (Grant No. IT1470-22) and Grant No. PGC2018-101355-B-I00 funded by MCIN/AEI/10.13039/501100011033, the Ministry for Digital Transformation and Civil Service of the Spanish Government through the QUANTUM ENIA project call—Quantum Spain project, and by the European Union through the Recovery, Transformation and Resilience Plan-NextGenerationEU within the framework of the Digital Spain 2026 Agenda.

DATA AVAILABILITY

All data supporting the results of this work are included within the article itself, with full analytical derivations and proofs.

Appendix A: Deviation from Partial Swap for Correlated Initial States

For factorized initial states $\rho_{SE}(0) = \rho_S \otimes \rho_E$, the reduced system Bloch vector obeys Eq. (24),

$$\vec{s}(t) = c^2 \vec{s} + d^2 \vec{e} + 2cd (\vec{s} \times \vec{e}), \quad (\text{A1})$$

which depends only on (\vec{s}, \vec{e}) and the Heisenberg parameters (c, d) .

For correlated initial states, it is convenient to use the full Bloch decomposition

$$\rho_{SE}(0) = \frac{1}{4} \left(\mathbb{I} \otimes \mathbb{I} + \vec{s} \cdot \vec{\sigma} \otimes \mathbb{I} + \mathbb{I} \otimes \vec{c} \cdot \vec{\sigma} + \sum_{j,k} C_{jk} \sigma_j \otimes \sigma_k \right), \quad (\text{A2})$$

where $C_{jk} = \text{Tr}[\rho_{SE}(0) \sigma_j \otimes \sigma_k]$ is the correlation tensor. For product states one has $C_{jk} = s_j e_k$, so we write

$$C_{jk} = s_j e_k + T_{jk}, \quad (\text{A3})$$

where T is a real 3×3 matrix that vanishes if and only if $\rho_{SE}(0)$ is factorized.

Evolving $\rho_{SE}(0)$ under $U(t) = e^{-iH_{\text{ext}}t}$ and tracing out E yields

$$\vec{s}(t) = \vec{s}_{\text{pswap}}(t) + \vec{\delta}(t), \quad (\text{A4})$$

where $\vec{s}_{\text{pswap}}(t)$ is the partial-swap expression in Eq. (A1) (coming from the $s_j e_k$ part), and

$$\delta_j(t) = \sum_{k,\ell} K_{jk\ell}(t) T_{k\ell}, \quad (\text{A5})$$

for some real coefficients $K_{jk\ell}(t)$ determined by H_{ext} . Thus $\vec{\delta}(t) = 0$ for all factorized states (since $T = 0$), and $\vec{s}(t)$ is constrained to the partial-swap family. For correlated initial states ($T \neq 0$), the deviation term $\vec{\delta}(t)$ can drive $\vec{s}(t)$ away from that family.

Our witness is precisely sensitive to such deviations: if for some time t^* the measured $z(t^*) = s_z(t^*)$ lies outside the factorized envelope derived from Eq. (A1), then necessarily $T \neq 0$, and the initial state $\rho_{SE}(0)$ cannot be written as a product.

-
- [1] H.-P. Breuer and F. Petruccione, *The Theory of Open Quantum Systems* (Oxford University Press, 2002).
 - [2] R. Alicki and K. Lendi, *Quantum Dynamical Semigroups and Applications* (Springer, 2007).
 - [3] P. Pechukas, Physical Review Letters **73**, 1060 (1994).
 - [4] R. Alicki, Physical Review Letters **75**, 3020 (1995).
 - [5] A. Shaji and E. C. G. Sudarshan, Physics Letters A **341**, 48 (2005).
 - [6] E.-M. Laine, J. Piilo, and H.-P. Breuer, Physical Review A **81**, 062115 (2010).
 - [7] K. Modi, A. Brodutch, H. Cable, T. Paterek, and V. Vedral, Reviews of Modern Physics **84**, 1655 (2012).
 - [8] Y.-Y. Xie, Z.-M. Wang, and L.-A. Wu, Fault-tolerant universal quantum computing in the presence of anisotropic noise (2025), arXiv:2508.04892, arXiv:2508.04892 [quant-ph].
 - [9] R. Horodecki, P. Horodecki, M. Horodecki, and K. Horodecki, Reviews of Modern Physics **81**, 865 (2009).
 - [10] M. Ringbauer, C. J. Wood, K. Modi, A. Gilchrist, A. G. White, and A. Fedrizzi, Physical Review Letters **114**, 090402 (2015).
 - [11] A. Smirne, D. Brivio, S. Cialdi, B. Vacchini, and M. G. Paris, Physical Review A **84**, 032112 (2011).
 - [12] M. Gessner and H.-P. Breuer, Physical Review Letters **107**, 180402 (2011).
 - [13] J. Dajka, M. Mierzejewski, and J. Luczka, Physical Review A **84**, 012103 (2011).
 - [14] S. Wißmann, B. Vacchini, and H.-P. Breuer, Physical Review A **88**, 022108 (2013).
 - [15] C.-F. Li, J.-S. Tang, Y.-L. Li, and G.-C. Guo, Physical Review A **83**, 064102 (2011).
 - [16] M. Gessner, M. R. Barbosa, A. S. V. Khoury, D. Frustaglia, and H.-P. Breuer, Nature Physics **10**, 105 (2014).
 - [17] E. Chitambar, M.-H. Hsieh, and F.-W. Shu, Physical Review Letters **115**, 060402 (2015).
 - [18] M. S. Byrd, F.-W. Shu, and E. Chitambar, Physical Review A **93**, 052101 (2016).
 - [19] I. Sargolzhai, Physical Review A **109**, 022213 (2024).
 - [20] G. Zhu, D. Qu, L. Xiao, and P. Xue, Photonics **9**, 883 (2022).
 - [21] L. Amico, R. Fazio, A. Osterloh, and V. Vedral, Reviews of Modern Physics **80**, 517 (2008).
 - [22] L. M. K. Vandersypen and I. L. Chuang, Reviews of Modern Physics **76**, 1037 (2005).
 - [23] O. Hagen and M. S. Byrd, Physical Review A **104**, 042406 (2021).
 - [24] R. R. Ceballos, *G-Consistent Subsets and Reduced Dynamical Quantum Maps*, Ph.d. dissertation, Southern Illinois University Carbondale (2017).